# RESEARCH PAPER

# The local anaesthetics proadifen and adiphenine inhibit nicotinic receptors by different molecular mechanisms

Guillermo Spitzmaul[1], Fernanda Gumilar[1], James P Dilger[2] and Cecilia Bouzat[1]

[1]*Instituto de Investigaciones Bioquímicas, Universidad Nacional del Sur-CONICET, Camino La Carrindanga Km 7, Bahía Blanca, Argentina, and* [2]*Department of Anesthesiology, Stony Brook University, Stony Brook, NY, USA*

**Background and purpose:** Many local anaesthetics are non-competitive inhibitors of nicotinic receptors (acetylcholine receptor, AChR). Proadifen induces a high-affinity state of the receptor, but its mechanism of action and that of an analogue, adiphenine, is unknown.

**Experimental approach:** We measured the effects of proadifen and adiphenine on single-channel and macroscopic currents of adult mouse muscle AChR (wild-type and mutant). We assessed the results in terms of mechanisms and sites of action.

**Key results:** Both proadifen and adiphenine decreased the frequency of ACh-induced single-channel currents. Proadifen did not change cluster properties, but adiphenine decreased cluster duration (36-fold at $100\,\mu mol \cdot L^{-1}$). Preincubation with proadifen decreased the amplitude ($IC_{50} = 19\,\mu mol \cdot L^{-1}$) without changing the decay rate of macroscopic currents. In contrast, adiphenine did not change amplitude but increased the decay rate ($IC_{50} = 15\,\mu mol \cdot L^{-1}$). Kinetic measurements demonstrate that proadifen acts on the resting state to induce a desensitized state whose kinetics of recovery resemble those of ACh-induced desensitization. Adiphenine accelerates desensitization from the open state, but previous application of the drug to resting receptors is required. Both drugs stabilize desensitized states, as evidenced by the decrease in the number of clusters elicited by high ACh concentrations. The inhibition by adiphenine is not affected by proadifen, and the mutation αE262K decreases the sensitivity of the AChR only for adiphenine, indicating that these drugs act at different sites.

**Conclusions and implications:** Two analogous local anaesthetics bind to different sites and inhibit AChR activity via different mechanisms and conformational states. These results provide new information on drug modulation of AChR.

*British Journal of Pharmacology* (2009) **157,** 804–817; doi:10.1111/j.1476-5381.2009.00214.x; published online 30 April 2009

## Introduction

The nicotinic acetylcholine receptor (AChR) is a ligand-gated ion channel (LGIC), member of the Cys-loop receptor super-family (Sine and Engel, 2006; Changeux and Taly, 2008). It is a pentamer of homologous subunits with composition $(\alpha 1)_2 \beta 1 \epsilon \delta$ in adult muscle. AChRs can be found in different conformational states: resting but able to be activated, which is more stable in the absence of agonist and has low affinity for agonists; open, which is transient and stabilized by the presence of agonist; and desensitized, which predominates after a prolonged exposure to the agonist and shows high affinity. There are several desensitized states that depend on the time of exposure to the agonist and that show different kinetics of recovery to the resting state (Elenes and Auerbach, 2002). The transitions between closed, open and desensitized states are affected by agonists and competitive antagonists, acting at the ACh-binding sites, and by a broad class of non-competitive inhibitors (NCIs) (Arias *et al.*, 2006). These inhibitors act by different general mechanisms: steric block-ade of the ion pore, allosteric inhibition of the channel or enhancement of desensitization. For most NCIs, the relation-ship between their chemical structures and their sites of inter-action and mechanisms of action has been particularly difficult to understand.

In addition to their well-known peripheral effects mediated by their action at voltage-sensitive $Na^+$ channels (Catterall and Mackie, 2001), local anaesthetics have been shown to modu-late LGICs. These channels have been investigated as potential targets of local anaesthetics in the brain, and therapeutic applications of local anaesthetics may produce peak plasma and/or brain concentrations capable of inducing significant functional inhibition of LGIC (Gentry and Lukas, 2001).

Inhibition of AChR by local anaesthetics
G Spitzmaul *et al*
805

However, the mechanisms of action and sites of interaction of local anaesthetics on LGICs are not as well understood.

Proadifen, meproadifen and adiphenine are closely related local anaesthetics. Early studies have shown that proadifen increases the agonist affinity of *Torpedo californica* AChR and this was interpreted in terms of a stabilization of the desensitized state (Heidmann *et al.*, 1983; Boyd and Cohen, 1984). Using infrared difference spectroscopy, Ryan *et al.* (2001) demonstrated that by binding to its NCI site, proadifen stabilizes a conformational state of *T. californica* AChR that has some, but not all of the features of the desensitized state. Other local anaesthetics, such as adiphenine and tetracaine, have been shown to decrease the affinity of the AChR for ACh, which has been interpreted as shifting the equilibrium in favour of the resting state (Boyd and Cohen, 1984). In addition to binding to the NCI site, proadifen and adiphenine have been shown to interact with the neurotransmitter-binding sites at higher concentrations.

Thus, despite these early studies and the wide use of proadifen as a tool for stabilizing the desensitized state of the muscle AChR (Prince and Sine, 1999), the molecular mechanisms underlying the modulation by proadifen and related drugs are not clear.

In the present study we explored in detail the functional effects of proadifen and its analogue adiphenine on adult mouse skeletal muscle AChR at both single-channel and macroscopic current levels. We showed that despite being chemically similar, the mechanisms of action of these local anaesthetics and the conformational states affected are completely different. In addition, our results suggest that their non-competitive binding sites in the muscle AChR are different.

## Methods

### Expression of AChR

Human embryonic kidney (HEK) 293 cells were transfected with adult mouse skeletal muscle α1(wild-type or mutant), β1, δ and ε cDNA subunits using calcium phosphate precipitation at a subunit ratio of 2:1:1:1 for α:β:δ:ε respectively (Bouzat *et al.*, 1994; 1998). The subunit nomenclature conforms to *BJP*'s Guide to Receptors and Channels (Alexander *et al.*, 2008). Mutant αE262K subunit was constructed by using the QuikChange site-directed mutagenesis kit. Restriction mapping and DNA sequencing confirmed the construct. Position number corresponds to that of *T. californica* AChR. Cells were used for electrophysiological measurements 1 or 2 days after transfection.

### Patch-clamp recordings

Single-channel currents were recorded in the cell-attached or outside-out patch configurations, and macroscopic currents were recorded in the outside-out patch configuration (Hamill *et al.*, 1981) at 20°C.

*Cell-attached patch recordings.* For cell-attached patches the bath and pipette solutions contained (in mmol·L$^{-1}$): KCl 142, NaCl 5.4, CaCl$_2$ 1.8, MgCl$_2$ 1.7 and HEPES 10 (pH 7.4). Patch pipettes were pulled from 7052 capillary tubes and coated with Sylgard. ACh, proadifen and adiphenine were added to the pipette solution. Single-channel currents were recorded using an Axopatch 200 B patch-clamp amplifier, digitized at 5 µs intervals with the PCI-6111E interface, recorded to the computer hard disk using the Acquire programme and detected by the half-amplitude threshold criterion using the TAC 4.0.10 programme at a final bandwidth of 10 kHz unless noted otherwise. Unless specified, single-channel currents from cell-attached patches were measured at an applied pipette potential of 70 mV. With the bath and pipette solutions here used, the resting potential approaches zero, and therefore the membrane potential is close to the pipette potential but with opposite sign. Open- and closed-time histograms were plotted by using a logarithmic abscissa and a square root ordinate and fitted to the sum of exponential functions by maximum likelihood using the TACFit programme. Clusters of openings corresponding to a single channel were identified as a series of closely spaced events preceded and followed by closed intervals greater than a specified duration ($\tau_{crit}$). This duration was taken as the point of intersection of the predominant closed component and the succeeding one in the closed time histogram. Cluster duration histograms were constructed setting the burst resolution time to that corresponding to $\tau_{crit}$ (Bouzat *et al.*, 2000).

*Outside-out patch recordings.* For outside-out patch recordings, the pipette solution contained (in mmol·L$^{-1}$): KCl 134, EGTA 5, MgCl$_2$ 1 and HEPES 10 (pH 7.3). Extracellular (bath) solution contained (in mmol·L$^{-1}$): NaCl 150, CaCl$_2$ 1.8, MgCl$_2$ 1 and HEPES 10 (pH 7.3). The patch was excised in this configuration and moved into position at the outflow of a perfusion system (Liu and Dilger, 1991; Demazumder and Dilger, 2001; Spitzmaul *et al.*, 2001). The perfusion system allows for a rapid (0.2–1 ms) exchange of the solution bathing the patch.

For single-channel recordings in the outside-out patch configuration, we used a three-tube perfusion system. One tube contained bath solution, the second tube bath solution with ACh, and the third one bath solution with ACh and the local anaesthetic. First, we applied the solution containing ACh for 30–60 s, then washed the patch for 1 min with bath solution and finally applied the solution containing ACh and local anaesthetic for 30–60 s. Recordings were obtained at an applied pipette potential of –50 mV.

For macroscopic currents in the outside-out configuration, we used a two-tube perfusion system. A series of applications of 300 µmol·L$^{-1}$ ACh (200 ms) were first applied to the patch at 5 s intervals. We then recorded the responses using different protocols: (i) (+/–) protocol: constant exposure to bath solution containing a specified concentration of the drug followed by a 200 ms pulse of 300 µmol·L$^{-1}$ ACh; (ii) (+/+) protocol: ≥2 min exposure to bath solution containing a specified concentration of the drug followed by a 200 ms pulse of bath solution containing ACh plus the same concentration of the drug; and (iii) (–/+) protocol: constant exposure to bath solution followed by a 200 ms pulse of bath solution containing 300 µmol·L$^{-1}$ ACh plus the drug. After each protocol, drug-free solutions were applied again to assess loss of channel activity. Unless specified, pipette potential was –50 mV.

Macroscopic currents were filtered at 5 kHz, digitized at 20 kHz and stored on the hard disk. Data analysis was performed by using the IgorPro software. The ensemble mean current was calculated for 10 individual current traces. Mean currents were fitted by a single exponential function:

$$I_{(t)} = I_0 \exp(-t/\tau) + I_{SS} \qquad (1)$$

where $I_0$ and $I_{ss}$ are the peak and the steady state current values, respectively, and $\tau$ is the decay time constant that measures the current decay. At high agonist concentration, the decay of macroscopic currents is mainly due to desensitization because the concentration of agonist is saturating, the probability of channel opening ($P_o$) is high, and the recovery from desensitization in the presence of agonist is slow. Current records were aligned with each other at the point where the current had risen to 50% of its maximum level. Peak currents correspond to the value obtained by extrapolation of the decay current to this point.

Fractional inhibition of peak current by proadifen was calculated as the ratio of the current in the presence of proadifen, $I_D$, to the control current, $I_C$. Fractional decrease of decay time constant was determined as the ratio in the presence of adiphenine, $\tau_D$ to that of control, $\tau_C$. These ratios were plotted as a function of NCI concentration, and the curves were fit to the Hill equation:

$$I_D/I_C \text{ (or } \tau_D/\tau_C) = IC_{50}{}^{nH}/(IC_{50}{}^{nH} + [NCI]^{nH}) \qquad (2)$$

where [NCI] is the concentration of proadifen or adiphenine, $IC_{50}$ is the concentration for 50% inhibition, and $n_H$ is the Hill coefficient.

To measure the kinetics of inhibition and recovery of AChR currents a three-tube perfusion system was used (Demazumder and Dilger, 2001). Tube 1 contained bath solution, tube 2 contained 300 µmol·L$^{-1}$ ACh, and tube 3 contained proadifen, or 300 µmol·L$^{-1}$ ACh or 300 µmol·L$^{-1}$ ACh plus proadifen. Initially, bath solution flowing through tube 1 was applied to the patch. Current responses were measured by using a test pulse that consisted on a 200 ms application of 300 µmol·L$^{-1}$ ACh (tube 2). After seven test pulses (tube 2), the patch was exposed to 13 pulses of the solution contained in tube 3 (~30 s) and then the control protocol was resumed. Relative peak currents were calculated and the onset/recovery phases were fitted to a single exponential decay function.

Experimental data are shown as mean ± s.d. Statistical comparisons were done by using Student's $t$-test. A level of $P < 0.05$ was considered significant.

### Simulation of macroscopic currents

Simulation of macroscopic currents in the presence of adiphenine was performed by using the software from QuB Suite (State University of New York, Buffalo) as described (Gumilar et al., 2003). The concentration of ACh was 300 µmol·L$^{-1}$. Binding, gating and desensitization rate constants were fixed to previously determined values (Bouzat et al., 2000; 2002). The values were: $k_{+1} = 300$ µM$^{-1}$·s$^{-1}$; $k_{-1} = 27\,000$ s$^{-1}$; $k_{+2} = 150$ µM$^{-1}$·s$^{-1}$; $k_{-2} = 54\,000$ s$^{-1}$; $\beta_2 = 50\,000$ s$^{-1}$; $\alpha_2 = 1000$ s$^{-1}$; $d_{+2} = 45$ s$^{-1}$; $d_{-2} = 0.2$ s$^{-1}$ (see Scheme 1). The forward blocking constant for adiphenine, $k_{+b}$, was set at $5 \times 10^6$ M$^{-1}$·s$^{-1}$, the value that correctly predicts the adiphenine concentration dependence of the macroscopic current decay time constant at 300 µmol·L$^{-1}$ ACh. The unblocking constant rate, $k_{-b}$, was allowed to vary, and the simulated currents were analysed by using IGOR Pro software and fitted by Equation 1.

### Materials

The QuikChange site-directed mutagenesis kit was obtained from Strategene (USA); 7052 capillary tubes, Garner Glass (CA, USA); Sylgard, Dow Corning (Midland, MI, USA); Axopatch 200 B patch-clamp amplifier, Axon Instruments Inc. (CA, USA); PCI-6111E Interface, National Instruments (Austin, TX, USA); Acquire programme, TAC 4.0.10 programme and TACFit programme, Bruxton Corporation (Seattle, WA, USA); IgorPro software, WaveMetrics Inc. (Lake Oswego, OR, USA).
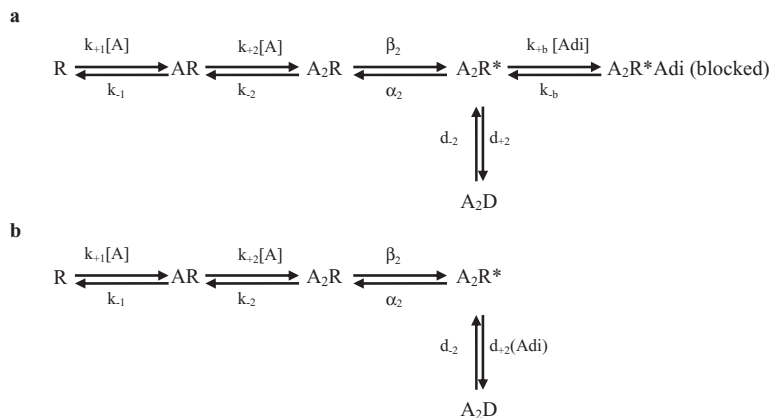


**Scheme 1** General model of activation, desensitization and open-channel block of the acetylcholine receptor (AChR). Receptor states are denoted by R (resting, closed), AR (1 ACh bound, closed), $A_2R$ (2 ACh bound, closed), $A_2R^*$ (2 ACh bound, open), $A_2R^*Adi$ (2 ACh bound, open but blocked by adiphenine) and $A_2D$ (2 ACh bound, desensitized). The rate constants used in simulations are listed in *Methods*. For the model in which adiphenine accelerates desensitization (b), the $d_{+2}$ rate constant is considered to be a function of adiphenine concentration.

Inhibition of AChR by local anaesthetics
G Spitzmaul *et al*
807

## Results

*Effects of proadifen and adiphenine on single-channel currents*

In order to evaluate the influence of proadifen and adiphenine on channel activation, single channels were activated by 30 μmol·L$^{-1}$ ACh to produce clear clusters in cell-attached patches. This concentration of ACh was chosen because it is close to the EC$_{50}$ for adult muscle AChR (Bouzat *et al.*, 2000) and is, therefore, sensitive to changes in activation parameters. Each activation period (cluster) begins with the transition of a single receptor from the desensitized to the open state and terminates by returning to the desensitized state (Figure 1A) (Sakmann *et al.*, 1980; Salamone *et al.*, 1999). At 30 μmol·L$^{-1}$ ACh, open time histograms show a main open component of about 1 ms (Figure 1A, right panel). Closed time histograms exhibit a major intermediate component of

about 1.5 ms that was sensitive to ACh concentration and corresponds to closings within clusters (Bouzat *et al.*, 2000). Cluster duration histograms show a main long duration component of about 110 ms whose relative area is larger than 0.7, and a brief component that corresponds to isolated openings (Figure 1A, right panel).

The mean duration of the open (MOT) and the intracluster closed (MCT) components as well as the cluster duration (MCluD) were unchanged when proadifen was included in the patch pipette (Figure 1). However, there was a large concentration-dependent decrease in the number of clusters, and therefore concentrations of proadifen higher than 20 μmol·L$^{-1}$ could not be tested. In contrast, in the presence of adiphenine, a concentration-dependent reduction of the cluster duration was observed (Figure 1). This reduction was accompanied by a decrease in the number of opening events
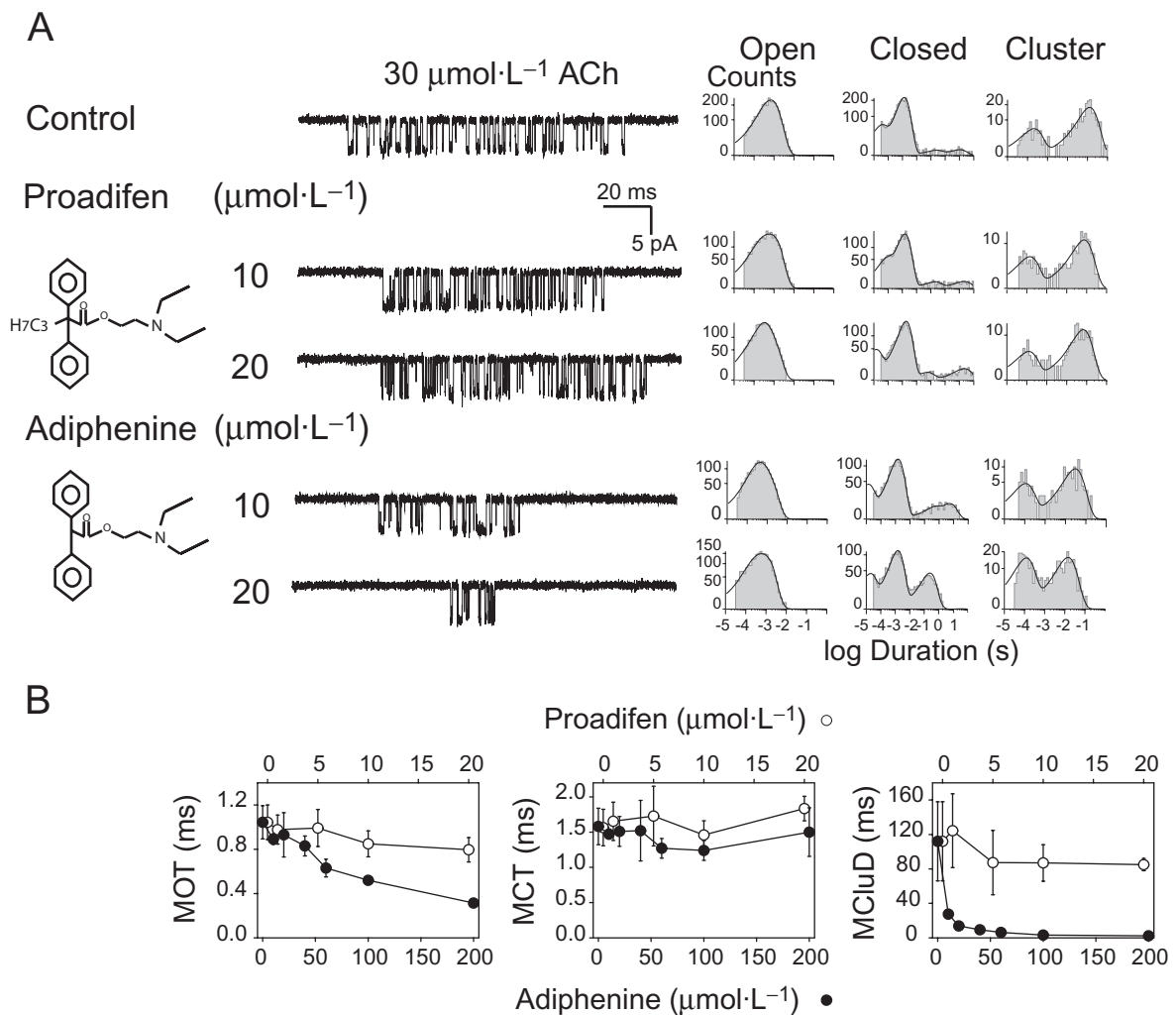


**Figure 1** Effect of local anaesthetics on single-channel kinetics. (A) Left panel: clusters of single-channel currents activated by 30 μmol·L$^{-1}$ acetylcholine (ACh) in the absence and presence of the indicated concentrations of proadifen or adiphenine. Channels were recorded in the cell-attached patch configuration. Currents are displayed at a bandwidth of 9 kHz with channel openings as downward deflections. Pipette potential: 70 mV. Right panel: open-, closed- and cluster-duration histograms corresponding to AChRs recorded at the local anaesthetic concentration indicated on the left. (B) Dependence of mean open time (MOT), mean closed time (MCT) and mean cluster duration (MCluD) on proadifen and adiphenine concentration. In all panels the labels of the top and bottom *x*-axis correspond to proadifen and adiphenine concentrations respectively. Data were obtained from the corresponding histograms and are shown as mean ± s.d. of at least three different recordings.

within clusters ($54 \pm 24$ and $2.5 \pm 0.5$ openings per cluster in the absence and presence of $200\ \mu mol \cdot L^{-1}$ adiphenine respectively; Figure 1). The mean open time remained constant up to $40\ \mu mol \cdot L^{-1}$ adiphenine and showed a concentration-dependent decrease at higher concentrations (Figure 1B). The duration of the major closed component also remained constant at all adiphenine concentrations but its relative area decreased from $0.72 \pm 0.08$ to $0.15 \pm 0.03$ at $200\ \mu mol \cdot L^{-1}$ adiphenine (Figure 1). This decrease is due mainly to the decrease in the number of opening events within clusters. As a result, the longer closed intervals become more prominent in the histograms. As for proadifen, a significant decrease in the number of clusters in the presence of adiphenine was observed.

Neither proadifen nor adiphenine affected the channel amplitude. At a pipette potential of 70 mV, the amplitudes were $5.4 \pm 0.2$, $5.3 \pm 0.4$ and $5.2 \pm 0.3$ pA for control, $20\ \mu mol \cdot L^{-1}$ proadifen and $200\ \mu mol \cdot L^{-1}$ adiphenine respectively.

Given that single-channel recordings in the presence of proadifen and adiphenine showed a reduced number of channel openings, we measured the number of activation episodes on outside-out patches before and after applying local anaesthetics. AChRs were activated by two concentrations of ACh: $0.5\ \mu mol \cdot L^{-1}$, which is lower than the $EC_{50}$ and at which receptors are mainly in the closed state (Dilger and Brett, 1990; Bouzat et al., 2000) and, $100\ \mu mol \cdot L^{-1}$, which is higher than the

$EC_{50}$, and at which receptors show high desensitization (Auerbach and Akk, 1998; Corradi et al., 2007).

When $0.5\ \mu mol \cdot L^{-1}$ ACh was applied to outside-out patches, single-channel openings appeared as isolated events (Figure 2A, control). We first counted the number of openings within the interval 10–60 s after exposure to the agonist (Table 1). After a 1 min wash with an ACh-free solution, the patch was exposed to $0.5\ \mu mol \cdot L^{-1}$ ACh solution containing $20\ \mu mol \cdot L^{-1}$ proadifen or $60\ \mu mol \cdot L^{-1}$ adiphenine (Figure 2A). Proadifen reduced the frequency of channel openings measured for the interval 10–30 s after ACh + drug application ~140-fold (Table 1). For adiphenine, we counted the number of opening events during the interval 30–60 because the onset of inhibition appeared to be slower than that of proadifen. Adiphenine also decreased the frequency of opening events, but the degree of reduction was significantly lower than that of proadifen (eightfold reduction at $60\ \mu mol \cdot L^{-1}$ adiphenine) (Table 1). As a control, after a 1 min wash with drug-free solution, ACh was applied again to ensure that the number of openings did not decrease in the absence of the local anaesthetics. Because $0.5\ \mu mol \cdot L^{-1}$ ACh activates AChR with a low probability of opening, these experiments suggest that both drugs affect the closed state of the AChR and that proadifen produces a more profound decrease in channel activity than adiphenine.

To determine the effect of the local anaesthetics on the desensitized state of the receptor, we performed similar
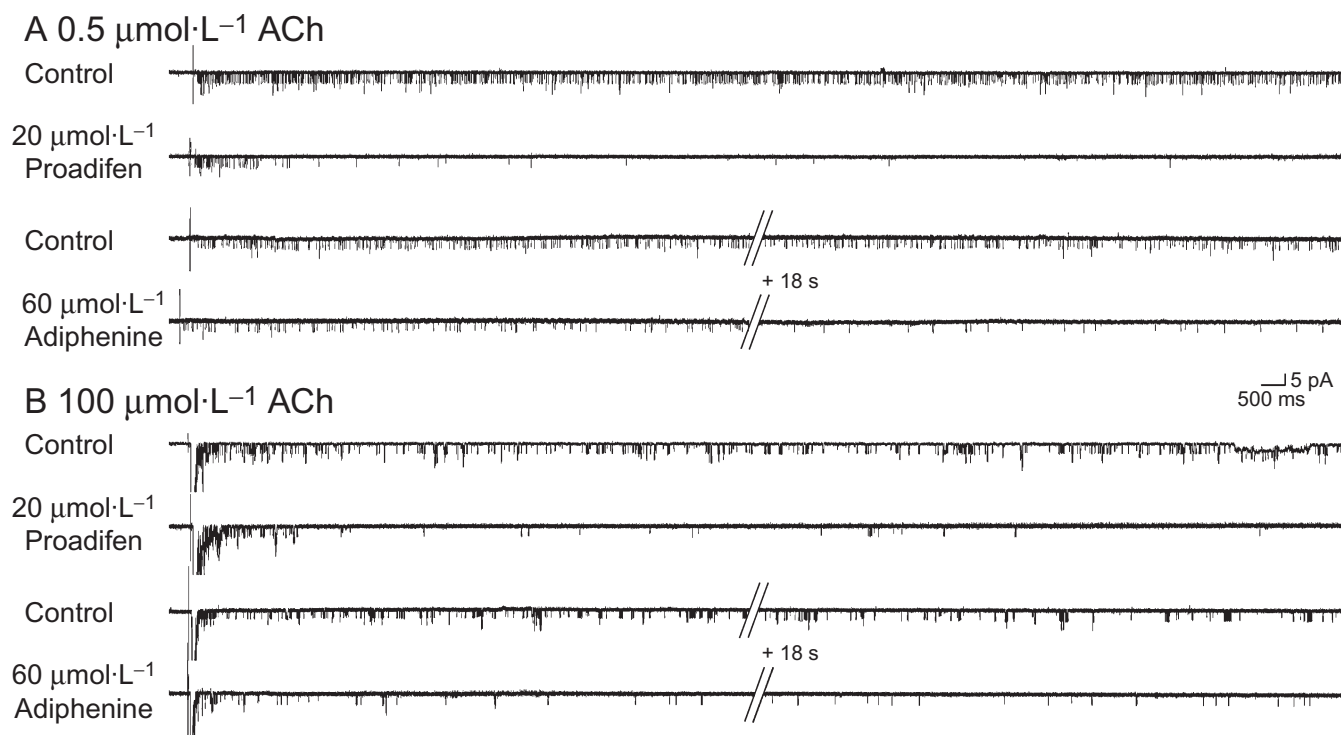


**Figure 2** Effect of local anaesthetics on single-channel activity of acetylcholine receptor (AChR) activated by low or high concentrations of ACh. Activation episodes of AChRs activated by 0.5 (A) or $100\ \mu mol \cdot L^{-1}$ ACh (B) in the absence (control trace) or presence of $20\ \mu mol \cdot L^{-1}$ proadifen or $60\ \mu mol \cdot L^{-1}$ adiphenine. AChR channels were recorded from outside-out patches at a pipette potential of $-50$ mV. Currents are displayed at a bandwidth of 5 kHz. Channel openings are shown as downward deflections. Each control trace and the succeeding local anaesthetic trace were obtained on the same patch. For proadifen, each trace shows 24 s of continuous acquisition. For adiphenine, control and local anaesthetic traces show channel activity during the first 12 s and after 30 s of channel activation. Activation episodes correspond to isolated events ($0.5\ \mu mol \cdot L^{-1}$ ACh) or cluster events ($100\ \mu mol \cdot L^{-1}$ ACh).

**Table 1** Effect of local anaesthetics on the frequency of activation episodes

| ACh ($\mu mol \cdot L^{-1}$) | Local anaesthetic | Local anaesthetic ($\mu mol \cdot L^{-1}$) | $F_{ratio}$ | n |
|---|---|---|---|---|
| 0.5 | Proadifen | 20 | 0.007 ± 0.002 | 3 |
| 100 | Proadifen | 20 | 0.048 ± 0.019 | 3 |
| 0.5 | Adiphenine | 60 | 0.122 ± 0.088 | 3 |
| 100 | Adiphenine | 60 | 0.472 ± 0.161 | 4 |

The frequency of acetylcholine receptor (AChR) channel activation episodes were determined by using outside-out patches activated with low or high concentrations of ACh in the absence or presence of the local anaesthetic. For 0.5 $\mu mol \cdot L^{-1}$ ACh, activation episodes correspond to isolated openings and for 100 $\mu mol \cdot L^{-1}$ ACh, activation episodes correspond to clusters. Episodes were counted for 10–30 s and 30–60 s for proadifen and adiphenine respectively. $F_{ratio}$ is the ratio between the frequency in the presence of the local anaesthetic and the corresponding control frequency; *n* is the number of experiments for each condition.

experiments in the presence 100 $\mu mol \cdot L^{-1}$ ACh. Rapid application of 100 $\mu mol \cdot L^{-1}$ ACh produced a current that decayed within 150 ms (Figure 2B, control). After complete desensitization, clusters of channel openings, corresponding to AChRs that recover from desensitization, were observed (Figure 2B, control). When proadifen or adiphenine was present during the agonist pulse, the peak current remained almost unaffected, but the number of clusters observed after complete desensitization and measured for the 10–30 s (proadifen) or 30–60 s (adiphenine) interval was significantly reduced (Figure 2B and Table 1). Because 100 $\mu mol \cdot L^{-1}$ ACh induced high desensitization, these experiments suggest that the local anaesthetics stabilize the agonist-induced desensitized state, and, again, that the potency of proadifen to produce this effect is higher than that of adiphenine.

*Effects of local anaesthetics on macroscopic AChR currents*
*Inhibition of AChR currents as a function of local anaesthetic concentration.*   To gain more insights into the mechanism of inhibition of channel activity by proadifen and adiphenine, we studied the effect of the drugs on macroscopic currents recorded from outside-out patches rapidly perfused with 300 $\mu mol \cdot L^{-1}$ ACh. In the absence of local anaesthetic, control currents reached a peak between 0.2 and 1 ms and then decayed due to desensitization with a time constant of about 20 ms (Figure 3).

To study the concentration-dependent effects of proadifen and adiphenine, currents were recorded in the absence (–/– protocol) and in the continuous presence of the drugs (+/+ protocol, see *Methods*) (Figure 3). Proadifen decreased the peak current without changing the current decay rate (Figure 3A). Full recovery of control currents was obtained after removal of proadifen at all concentrations (Figure 3A). No currents were detected at proadifen concentrations higher than 60 $\mu mol \cdot L^{-1}$. A fit of the peak current inhibition curve (Figure 3A) to Equation 2 gave an $IC_{50} = 19 \pm 4 \mu mol \cdot L^{-1}$ ($n_H = 1.47 \pm 0.38$).

Adiphenine, in contrast to proadifen, had only a small effect on the extrapolated peak currents (25% decrease at 100 $\mu mol \cdot L^{-1}$). The main effect of adiphenine was to produce

a concentration-dependent decrease in the current decay time constant (Figure 3B; time constants were normalized to control). A fit of this plot to Equation 2 gave an $IC_{50} = 15 \pm 3 \mu mol \cdot L^{-1}$ ($n_H = 1.18 \pm 0.22$).

These results are consistent with the single-channel recordings that show that proadifen does not affect the cluster duration (a manifestation of the desensitization time constant), whereas adiphenine significantly reduces the cluster duration and may therefore act on the open state.

*Effects of local anaesthetic application protocol on inhibition of AChR.*   To investigate the state and time dependence of drug action, we used different perfusion protocols to expose AChRs to the local anaesthetics (see *Methods*). With 20 $\mu mol \cdot L^{-1}$ proadifen, both protocols in which drug was present before agonist application (+/+ and +/–) reduced the peak current by about 50% (Figure 4A). In contrast, when proadifen acts only on the open state (–/+ protocol) no changes in the peak current occur. The current decay rate was not significantly different from control for any application protocol. Similar effects were seen with 60 $\mu mol \cdot L^{-1}$ proadifen (Figure 4A).

When 300 $\mu mol \cdot L^{-1}$ ACh and 100 $\mu mol \cdot L^{-1}$ adiphenine were applied simultaneously (–/+ protocol), the decay rate was somewhat faster than control, but not as fast as when preincubation was employed (Figure 4B). Preincubation was necessary to increase the decay rate of AChR currents to its maximum value (Figure 4B, compare +/– and +/+ protocols). This suggests that the action of adiphenine on the open state of the channel has a slow onset. An explanation for this is that either the kinetics of binding are similar to the kinetics of desensitization or the drug must first bind to the closed state, therefore requiring preincubation to achieve its full action.

Acceleration of the current decay by 100 $\mu mol \cdot L^{-1}$ adiphenine was also seen when macroscopic currents were induced by 2 $\mu mol \cdot L^{-1}$ ACh (Figure 4C). Current decay is slower at lower agonist concentrations (Dilger and Liu, 1992). With 2 $\mu mol \cdot L^{-1}$ ACh alone, the decay was fit by a single exponential function with a time constant of 211 ± 37 ms ($n = 9$). When 100 $\mu mol \cdot L^{-1}$ adiphenine was present during activation (–/+ protocol), peak currents were not affected ($I_D/I_C = 1.10 \pm 0.14$) and currents decayed faster than the control but could still be fitted by a single exponential function ($\tau = 117 \pm 22$ ms). The fractional decrease of $\tau$ (0.56 ± 0.07) is similar to the fractional decrease seen at high ACh concentrations [0.53 ± 0.05 (Figure 4B)].

*Kinetics of inhibition by proadifen.*   To determine the rate at which proadifen interacts with the resting state of the channel, we used a three-tube perfusion protocol (see *Methods*). Peak current responses to 300 $\mu mol \cdot L^{-1}$ ACh were monitored as proadifen was rapidly introduced (onset) or removed (recovery) from the excised patch. Figure 5A illustrates the time course of inhibition and recovery after a 30 s exposure to proadifen. Single exponential fits of the relative current show that the onset of inhibition proceeds with time constants of 11, 6 and 4 s for 10, 15 and 30 $\mu mol \cdot L^{-1}$ proadifen respectively. For 60 $\mu mol \cdot L^{-1}$ proadifen, the peak current decreased more than 90% after a 2 s preincubation, making it impossible to obtain an accurate estimation of the onset rate. The recovery time constants were 6, 4, 3 and 3.2 s for 10, 15,
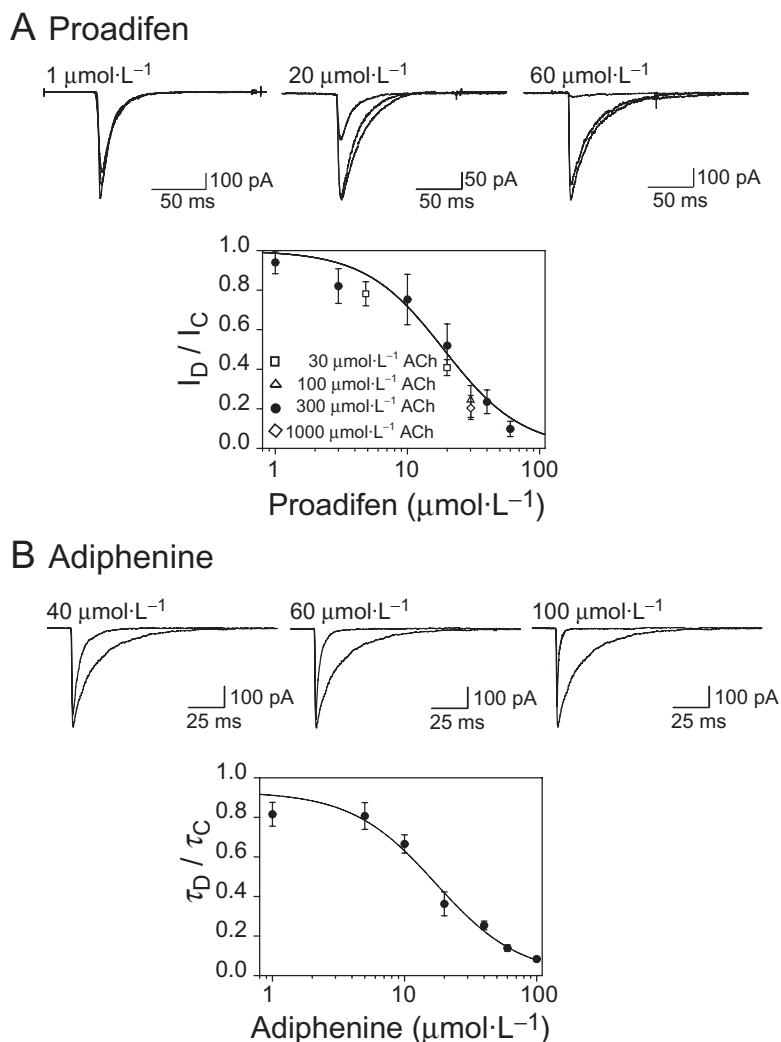
## A Proadifen



## B Adiphenine



**Figure 3** Macroscopic currents in the presence of different concentrations of local anaesthetic. Ensemble mean currents obtained in the outside-out configuration from rapid perfusion of acetylcholine (ACh) alone or in the continuous presence of proadifen (A) or adiphenine (B). Pipette potential of −50 mV. (A) Upper panel: macroscopic currents activated by 300 μmol·L$^{-1}$ ACh obtained in the presence of different concentrations of proadifen. For each concentration, control currents before and after proadifen application are shown. Lower panel: inhibition of the ACh receptor current by proadifen. $I_D/I_C$ is the relationship between the peak current obtained in the presence of proadifen ($I_D$) and the control current ($I_C$). Currents were activated by different concentrations of ACh as depicted in the figure. (B) Upper panel: Currents in the absence and presence of adiphenine. Lower panel: $\tau_D/\tau_C$ is the relationship between the decay time constant in the presence of adiphenine ($\tau_D$) and the control decay time constant ($\tau_C$). Each point represents the mean ± s.d. of at least three measurements. $\tau$-values were 23.1 ± 7.2 ms for control and 15.5 ± 5.0, 11.1 ± 2.0, 8.9 ± 3.0, 7.9 ± 1.7, 5.6 ± 0.7, 3.1 ± 0.7 and 1.8 ± 0.7 ms for 1, 5, 10, 20, 40, 60 and 100 μmol·L$^{-1}$ adiphenine respectively.

30 and 60 μmol·L$^{-1}$ proadifen respectively. The mean rate for the recovery from proadifen inhibition was 0.29 ± 0.05 s$^{-1}$. Figure 5B shows that onset of inhibition was concentration-dependent with a slope of 5 (±2) × 10$^3$ M$^{-1}$·s$^{-1}$ and recovery was concentration-independent because the slope, 2 (±3) × 10$^3$ M$^{-1}$·s$^{-1}$, was not significantly different from zero. These data, however, do not imply a first-order rate relationship because the onset rates are slower than the offset rates. Alternatively, the data suggest that a conformational change rather than the binding of proadifen is rate-limiting.

We performed a similar set of experiments to determine the rate at which desensitized channels recover from inhibition by proadifen. After establishing a baseline response to brief

applications of 300 μmol·L$^{-1}$ ACh, we exposed the patch to a 30 s application of 300 μmol·L$^{-1}$ ACh with or without proadifen. At the end of the 30 s period, brief applications of ACh were resumed to measure the time course of recovery from desensitization. When 300 μmol·L$^{-1}$ ACh alone was used in the desensitizing solution, currents recovered with a time constant of 3.8 ± 1.6 s (recovery rate: 0.29 ± 0.12 s$^{-1}$) (Figure 5B, 0 μmol·L$^{-1}$ proadifen). Similar results were seen when 10, 15, 30 or 60 μmol·L$^{-1}$ proadifen was included in the desensitizing solution (Figure 5B). The average rate at all concentrations was 0.30 ± 0.06 s$^{-1}$. Figure 5B demonstrates that recovery from inhibition by proadifen exposure to resting state channels and desensitized channels occur with the same
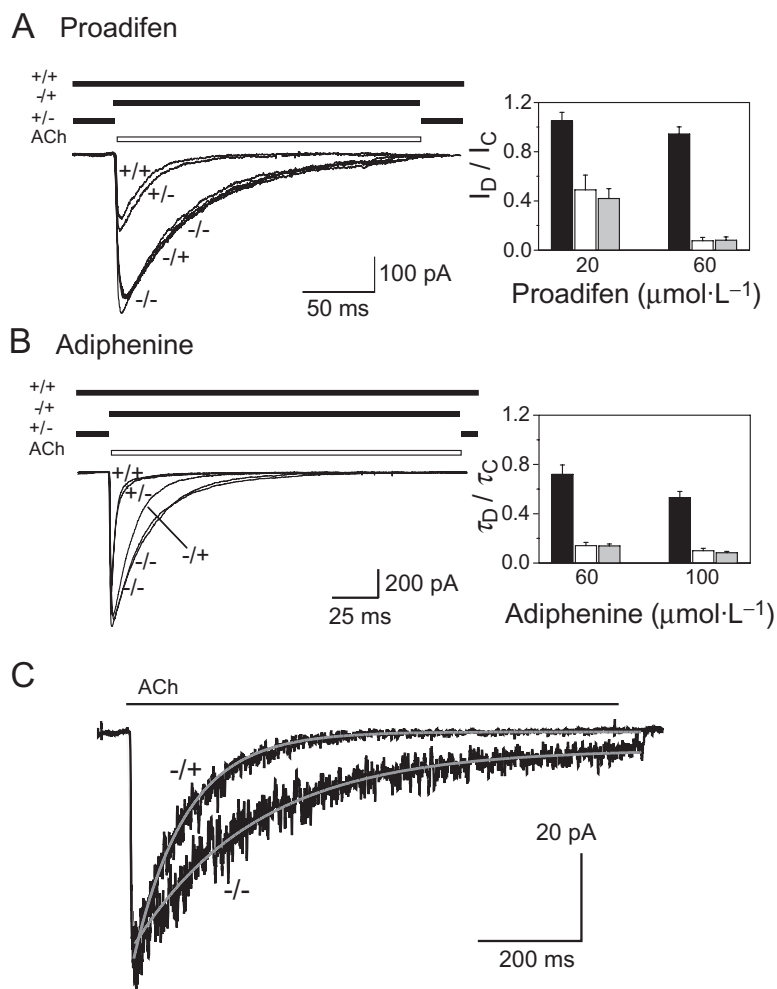
**Figure 4** Effect of local anaesthetic application protocol on macroscopic currents. (A) Left panel: superimposed current responses of outside-out patches to 300 μmol·L$^{-1}$ acetylcholine (ACh) and 20 μmol·L$^{-1}$ proadifen using the indicated application protocol: −/−, control condition (without drug); −/+, proadifen present only during activation; +/−, proadifen present only during 2 min preincubation and +/+, proadifen present during 2 min preincubation and activation. Right panel: inhibition of control currents ($I_C$) by proadifen ($I_D$) as a function of application protocol for 20 and 60 μmol·L$^{-1}$ proadifen. Open and hatched columns correspond to the presence of proadifen and the solid column shows ACh application for all protocols. (B) Left panel: current responses in the absence and presence of 100 μmol·L$^{-1}$ adiphenine using the indicated application protocol. Symbols are the same as in (A). Right panel: decrease of decay time constant ($\tau$) ratio as a function of application protocol for 60 and 100 μmol·L$^{-1}$ adiphenine. Key to columns as in (A). (C) Macroscopic currents were activated by 2 μmol·L$^{-1}$ ACh alone (−/− protocol) or in the simultaneous presence of 100 μmol·L$^{-1}$ adiphenine (−/+ protocol). Current decays were fits to a one-exponential function.

time course. Moreover, this is the same time course for recovery from desensitization by ACh. This supports the idea that proadifen induces a state that resembles the agonist-induced desensitized state.

*Effects of local anaesthetics as a function of potential.* In order to study the voltage dependence of local anaesthetic action, we recorded currents at different pipette potentials in the absence and presence of the drugs. We measured inhibition of peak macroscopic currents by proadifen between −90 and +90 mV (data not shown), There was a weak trend towards less inhibition at depolarized potentials but this was not statistically significant at 10 or 20 μmol·L$^{-1}$ proadifen. At 60 μmol·L$^{-1}$ proadifen, however, inhibition decreased e-fold for a 130 mV depolarization ($P = 0.03$). We also measured the decay time constant of macroscopic currents with

100 μmol·L$^{-1}$ adiphenine between −90 and +90 mV (data not shown). In agreement with published data (Dilger and Liu, 1992), the decay time constant of currents activated by saturating agonist concentrations was independent of voltage in the absence of drugs. With 100 μmol·L$^{-1}$ adiphenine, the time constants increased from $1.9 \pm 0.8$ ms at −90 mV to $3.9 \pm 1.7$ ms at +90 mV. The slope of the ln ($\tau$) versus V curve corresponded to an e-fold change in $\tau$ for 230 mV ($P = 0.015$). Thus, the actions of both local anaesthetics were only weakly voltage-dependent.

## Site of action of proadifen and adiphenine
*Interaction with the agonist-binding site.* To determine whether proadifen acts as a competitive antagonist at the concentrations studied here, we compared current inhibition in the
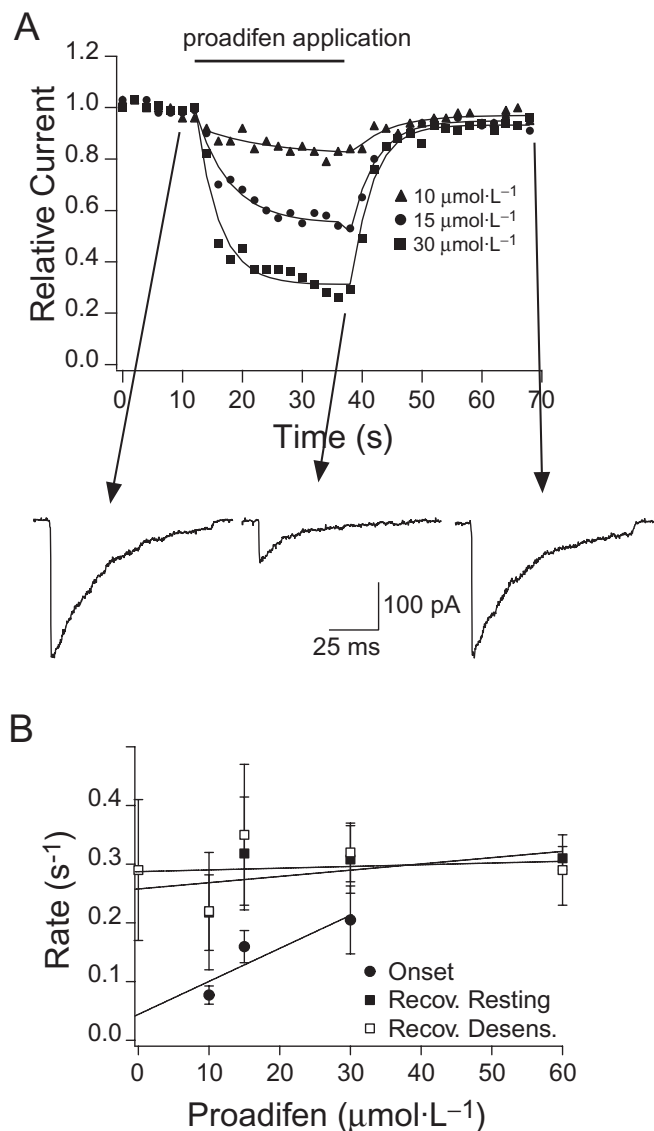
**Figure 5** The kinetics of inhibition of acetylcholine receptor (AChR) currents by proadifen. (A) ACh (300 µmol·L$^{-1}$) was applied at 2 s intervals. Proadifen at the specified concentration was introduced into the ACh-free solution after application #7 and removed after application #20. The time course of the normalized peak current was fit to single exponential functions to determine the onset and recovery time constants. Macroscopic current traces are shown at selected points for the 30 µmol·L$^{-1}$ proadifen experiment. (B) Summary of the onset and recovery (recov. resting) and full-agonist desensitized state (recov. densens) rates obtained from six patches with 2–5 determinations at each point. The individual data points were fit with linear regression.

continuous presence of proadifen using various concentrations of ACh. The results with 30–1000 µmol·L$^{-1}$ ACh are shown in Figure 3A. Thus, there is no evidence for competitive inhibition by proadifen concentrations ≤60 µmol·L$^{-1}$, and current inhibition arises mainly from the action of proadifen at its NCI-binding site rather than its action on the agonist-binding site.

To test whether adiphenine acts as a competitive antagonist we determined its effects on cluster duration as a function of

**Table 2** Cluster properties in the simultaneous presence of proadifen and adiphenine

| ACh (µmol·L$^{-1}$) | Proadifen (µmol·L$^{-1}$) | Adiphenine (µmol·L$^{-1}$) | Relative MCLuD | n |
|---|---|---|---|---|
| 30 | 0 | 10 | 0.19 ± 0.02 | 3 |
| 30 | 5 | 10 | 0.16 ± 0.02 | 5 |
| 30 | 15 | 10 | 0.15 ± 0.02 | 3 |
| 100 | 0 | 2 | 0.34 ± 0.05 | 3 |
| 100 | 15 | 2 | 0.28 ± 0.06 | 3 |

Data were obtained in the cell-attached configuration. Acetylcholine (ACh) (30 or 100 µmol·L$^{-1}$) was added to the pipette tip together with either adiphenine or adiphenine plus proadifen. Mean cluster duration (MCluD) was obtained from the corresponding histograms. *n* is the number of experiments for each condition.

ACh concentration. The fractional decrease in cluster duration by 10 µmol·L$^{-1}$ adiphenine was the same for 20, 30 and 100 µmol·L$^{-1}$ ACh (0.19 ± 0.04, 0.20 ± 0.04 and 0.20 ± 0.02 respectively). Adiphenine concentrations higher than 60 µmol·L$^{-1}$ (Figure 3B) slightly decreased the peak current that could be evidence for competitive antagonism. Although 100 µmol·L$^{-1}$ adiphenine decreased peak current by 25%, it has a much greater effect on cluster duration (97% decrease). Thus, the main effect observed for the action of adiphenine is mediated by its action at the NCI site.

*Combined effects of proadifen and adiphenine.* To investigate whether proadifen and adiphenine bind to the same NCI site, we examined whether the presence of proadifen modified the ability of adiphenine to decrease single-channel cluster duration. Cell-attached patch experiments were carried out using a pipette solution containing ACh, adiphenine and either 5 or 15 µmol·L$^{-1}$ proadifen. The decrease in cluster duration produced by adiphenine is not affected significantly by the presence of proadifen (Table 2).

*Effects of local anaesthetics on αE262 mutant AChR.* An analogue of proadifen, meproadifen mustard, labels residue αE262 in *T. californica* AChR (Pedersen *et al.*, 1992). This position is located in the extracellular ring of negatively charged residues of the ion pore (position 20′ of M2 domain) (Miyazawa *et al.*, 2003). It has been shown to contribute to channel conductance (Imoto *et al.*, 1988) and to participate in the binding site for the NCIs crystal violet (Arias *et al.*, 2006) and 3-azioctanol (Forman *et al.*, 2007). We therefore examined whether this position is involved in the action of proadifen or adiphenine in mouse AChR. To this end, we mutated αE262 to lysine and evaluated the effect of these local anaesthetics on the mutant AChRs.

Figure 6A shows macroscopic currents obtained from wild-type and mutant AChRs before and after preincubation with 20 and 60 µmol·L$^{-1}$ proadifen (left) and 40 and 100 µmol·L$^{-1}$ adiphenine (right). The decay time constants for wild-type and αE262K in the absence of drugs were not statistically different [19 ± 7.0 ms (*n* = 78) and 17.0 ± 6.4 ms (*n* = 26) respectively; *P* > 0.05]. Proadifen decreased the peak currents of the mutant AChR as a function of concentration (Figure 6A), but the degree of current inhibition by 20 and 60 µmol·L$^{-1}$ proadifen was similar in wild-type and mutant

Inhibition of AChR by local anaesthetics
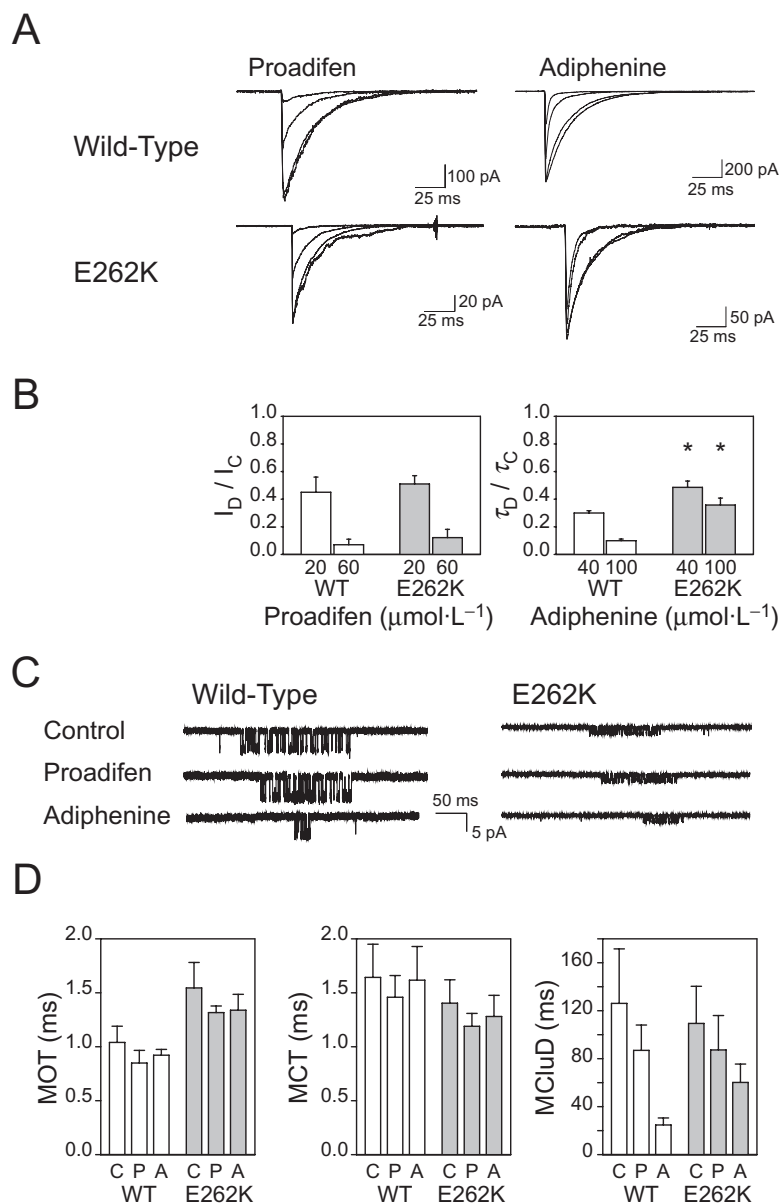G Spitzmaul *et al*
813

**Figure 6** Effect of local anaesthetics on acetylcholine receptor (AChR) mutated in αE262. (A) Superimposed macroscopic currents for wild-type and αE262K mutant AChRs in the absence and presence of 20 and 60 μmol·L$^{-1}$ proadifen (left panel) and 40 and 100 μmol·L$^{-1}$ adiphenine (right panel). Currents were recorded in the outside-out configuration and activated by 300 μmol·L$^{-1}$ ACh. (B) Inhibition of currents as a function of proadifen concentration (left) and decay time constant in the presence of adiphenine relative to control ($\tau_D/\tau_C$) (right) for wild-type (WT) and mutant αE262K AChRs. * Indicates statistically significant differences between wild-type and αE262K for each concentration. (C) Single-channel recordings of wild-type and αE262K mutant AChRs in the absence and presence of 10 μmol·L$^{-1}$ of either proadifen or adiphenine. Channels were recorded in the cell-attached patch configuration. Channel openings are shown as downward deflections. Pipette potential: 70 mV. Data for αE262K were filtered at 5 kHz. (D) Mean open time (MOT), mean closed time (MCT) and mean cluster duration (MCluD) for wild-type (WT) and αE262K AChRs in the absence (C) or presence of 10 μmol·L$^{-1}$ proadifen (P) or 10 μmol·L$^{-1}$ adiphenine (A). Data were taken from the corresponding histograms.

AChRs ($P > 0.05$ for 20 and 60 μmol·L$^{-1}$) (Figure 6B). These results suggest that in the mouse AChR, αE262 is not involved in the action of proadifen.

In the presence of 40 and 100 μmol·L$^{-1}$ adiphenine, the current decay rates of αE262K AChRs were slower than those of wild-type AChRs. The decay time constants for wild-type and αE262K AChRs were 5.6 ± 0.7 and 8.3 ± 1.2 ms (40 μmol·L$^{-1}$ adiphenine) and 1.8 ± 0.7 and 6.1 ± 1.0 ms

(100 μmol·L$^{-1}$ adiphenine). The differences in the current decay rates are statistically significant ($P < 0.05$) (Figure 6A and B). These results indicate that the αE262K mutation decreases the sensitivity of mouse AChR for adiphenine (Figure 6B).

To determine more clearly the consequences of the mutation αE262K on AChR inhibition by local anaesthetics, we studied the kinetics of activation at the single-channel level. Single-

channel amplitude was decreased by αE262K mutation (Figure 6C), as previously reported by Imoto *et al.* (1988). The measured amplitudes were 5.4 ± 0.2 and 2.2 ± 0.2 pA for wild-type and mutant αE262K AChR respectively. The mutation also caused a slight increase in the apparent mean open time but it did not affect significantly the closed and cluster durations (Figure 6D). In the presence of 10 µmol·L$^{-1}$ proadifen or adiphenine, αE262K channels were affected similarly to wild-type AChRs. However, in the presence of 10 µmol·L$^{-1}$ adiphenine, the magnitude of the decrease in the mean cluster duration was smaller for the mutant (twofold) than for the wild-type AChR (fivefold) (Figure 6C and D), again showing that this position affects only adiphenine interaction.

## Discussion and conclusions

In this study we identified the conformational states modulated by proadifen and adiphenine and described their mechanisms of action. We also determined that αE262 is involved in the sensitivity of the AChR for adiphenine but not for proadifen.

### Mechanism of AChR inhibition by proadifen
*Interaction of proadifen with the resting state.* At the single-channel level and in the presence of low ACh concentrations the main effect of proadifen was a great decrease in the frequency of channel openings (Figures 1 and 2A). Because under this condition a large proportion of closed dwell times correspond to resting AChRs (Dilger and Brett, 1990; Auerbach and Akk, 1998), such a decrease supports the idea that inhibition by the drug can occur from this state. In accordance with this, preincubation with proadifen induced maximal inhibition of macroscopic currents (Figure 4A). Similar effects have been reported for the proadifen analogue, meproadifen, which has been shown to reduce the frequency of opening events of AChRs in rat myoballs (Aracava and Albuquerque, 1984) and the peak amplitude of end-plate currents without affecting the current decay rate (Maleque *et al.*, 1982).

Onset of inhibition from the resting state is dependent on proadifen concentration whereas recovery is independent of it (Figure 5), suggesting that dissociation from the NCI site is faster than AChR re-isomerization to the resting state.

An alternative explanation for the decrease in the peak current could be competitive antagonism (Demazumder and Dilger, 2001; Wenningmann and Dilger, 2001). Proadifen is known to interact with the agonist-binding site in the *T. californica* AChR with an IC$_{50}$ between 300 and 600 µmol·L$^{-1}$ (Boyd and Cohen, 1984; Lurtz and Pedersen 1999). We showed that the effects of 1–30 µmol·L$^{-1}$ proadifen on macroscopic currents are not dependent on ACh concentration. Thus, the effect of proadifen at this range of concentration is mediated by binding at a non-competitive site and not at the agonist-binding site.

*Interaction of proadifen with the open state.* Inhibition by proadifen cannot be attributed to a decrease in open time, an appearance of a new closed state within clusters or an accel-eration of desensitization from the open state. In addition, proadifen did not increase the decay rate of macroscopic currents (Figure 3A) or modify peak macroscopic currents when applied simultaneously with ACh (Figure 4A). We cannot rule out the possibility that proadifen can inhibit open channels, but does so with slow kinetics (>100 ms).

*Interaction of proadifen with desensitized states.* Our experiments suggest that proadifen interacts with desensitized channels, as at a high ACh concentration (100 µmol·L$^{-1}$) closings between clusters correspond to dwell times in the desensitized state and proadifen decreases the number of clusters without affecting cluster duration. Different desensitized states have been reported for AChR (Elenes and Auerbach, 2002), but we cannot distinguish which state is stabilized by the drug.

Experiments on *T. californica* AChR showed that proadifen converts the receptor to a state of high affinity for ACh, comparable to the agonist-induced desensitized state (Boyd and Cohen, 1984; Prince and Sine, 1999). Ryan *et al.* (2001) determined that this high-affinity state is an intermediate between the resting and desensitized conformations of *Torpedo* AChR. We find that the rate of recovery from inhibition by proadifen occurs with a similar time course to recovery from ACh-induced desensitization (Figure 5B). Thus, if the proadifen-induced intermediate state identified by Ryan *et al.* (2001) is also present in mouse AChR, it cannot be distinguished kinetically from the fully desensitized state induced by ACh.

In summary, proadifen inhibits the AChR with slow kinetics, in the order of 0.3 s$^{-1}$. Inhibition via the closed and desensitized states can be detected after exposure to proadifen for several seconds. Given that the duration of channel opening is in the millisecond time scale, it is not possible to determine whether or not proadifen can inhibit the channel from the open state.

### Mechanism of AChR inhibition by adiphenine
*Interaction of adiphenine with the resting state.* At low ACh concentrations adiphenine decreased the frequency of opening events. Unlike proadifen, adiphenine did not decrease the amplitude of macroscopic currents but instead it increased the speed of current decay. However, adiphenine needs to be present prior to channel activation to produce its full effect on current decay. This has also been observed with NCIs such as 3-(trifluoromethyl)-3-(m-iodophenyl)diazirine (TID) (Forman, 1999) and quinacrine (Spitzmaul *et al.*, 2001). It is possible that adiphenine requires >10 ms to reach its NCI-binding site or that it binds to a site in the resting state, and after channel opening it rapidly moves to a second site from where it affects the open state. Our results are consistent with experiments on *T. californica* receptors showing that the preincubation with adiphenine increases the rate of conversion from the low- to the high-affinity conformation induced by agonists (Boyd and Cohen, 1984).

*Interaction of adiphenine with the open state.* The action of adiphenine on the open state was observed as an increase in the decay rate of macroscopic currents. The single-channel

mean open time also decreased with increasing concentrations of adiphenine. These observations are compatible with two mechanisms of action for adiphenine illustrated in Scheme 1: an increase in the intrinsic desensitization rate from the open state or a slow open-channel block. Although the mechanisms cannot be unequivocally distinguished, our results support the first one as the most probable mechanism.

The hallmarks of open-channel block are decreased single-channel open time ($MOT \propto 1/[blocker]$), the appearance of a new component in the closed time histogram (with a blocker concentration-independent time constant and concentration-dependent amplitude) and a two-exponential decay time in macroscopic currents (the fast component $\propto 1/[blocker]$, the slow component due to desensitization of unblocked channels). The concentration dependence of MOT suggests $k_{+b} = 9.0\ (\pm0.1) \times 10^6\ M^{-1}\cdot s^{-1}$, but adiphenine did not exhibit the other characteristics of open-channel block. If recovery from block ($k_{-b}$) is slow; however, desensitization may obscure the evidence for open-channel block (Papke and Oswald, 1989; Forman, 1999). In this scenario, clusters are terminated by a long-lasting block and the decay of macroscopic currents is dominated by the onset of block that is faster than desensitization. Our data can be used to place upper and lower limits on the speed of recovery from block. Using the (–/+) protocol in which receptors are exposed to drug during ACh application only, we find that there is no use dependence. The acceleration of current decay induced by adiphenine recovers during the 5 s interval between drug applications; thus, $k_{-b} > 1/2\ s = 0.5\ s^{-1}$. Using simulations of macroscopic currents the open-channel block model (see *Methods*; Scheme 1), we found that a two-component decay would not be apparent in macroscopic currents activated by either 300 $\mu mol\cdot L^{-1}$ ACh when $k_{-b} < 2\ s^{-1}$. Thus, there is a very narrow range of $k_{-b}$ values that could account for the adiphenine data in terms of open-channel block. In addition, the absence of a second exponential component in the decay of currents activated by low ACh concentrations suggests that open channel block is unlikely to be the cause of adiphenine inhibition (Figure 4C).

Consider the alternative interpretation of the effects of adiphenine, acceleration of desensitization. This model is illustrated in Scheme 1b with the block pathway removed and an adiphenine concentration-dependent forward rate constant for desensitization, $d_{+2}$(Adi). In this model, single-channel clusters will terminate sooner and macroscopic current decays will be faster as the rate of desensitization increases. These are qualitative predictions because the functional relationship between $d_{+2}$ and [Adi] is unknown. However, the apparent value of $d_{+2}$ at any [Adi] can be calculated from the mean cluster duration (MCluD) and cluster open probability ($P_o$): $d_{+2} = (MCluD \times P_o)^{-1}$ (Auerbach and Akk, 1998). These values are presented in Table 3. The MOT will also decrease in this model because there are two pathways for channel closure, $\alpha_2$ and $d_{+2}$; $MOT = (\alpha_2 + d_{+2})^{-1}$. Table 3 has the results of this calculation, and it can be seen that the predictions are in excellent agreement with the experimental data. Finally, the model also predicts that there will be no additional closed state components and a single exponential decay for macroscopic currents.

**Table 3** Prediction of mean open time as a function of adiphenine concentration

| Adiphenine ($\mu mol\cdot L^{-1}$) | Observed MOT (ms) | MCluD (ms) | $P_o$ | $d_{+2}$ ($s^{-1}$) | Predicted MOT (ms) |
|---|---|---|---|---|---|
| 0 | 0.99 | 116.0 | 0.37 | 23 | 0.98 |
| 10 | 0.92 | 24.7 | 0.32 | 130 | 0.89 |
| 20 | 0.93 | 13.7 | 0.31 | 230 | 0.81 |
| 40 | 0.83 | 9.3 | 0.32 | 340 | 0.75 |
| 60 | 0.63 | 6.3 | 0.30 | 540 | 0.65 |
| 100 | 0.52 | 3.2 | 0.27 | 1160 | 0.46 |
| 200 | 0.31 | 3.3 | 0.20 | 1530 | 0.39 |

Data were determined from single-channel recordings of acetylcholine receptors (AChRs) activated by 30 $\mu mol\cdot L^{-1}$ ACh. Observed mean open time (MOT) and mean cluster duration (MCluD) were obtained from the corresponding histograms. The apparent forward desensitization rate, $d_{+2}$, was calculated as $(MCluD \times P_o)^{-1}$. Predicted MOT was calculated as $1/(\alpha_2 + d_{+2})$. $\alpha_2 = 1000\ s^{-1}$. $P_o$ is the probability of channel opening within a cluster.

*Interaction of adiphenine with the desensitized state.* Adiphenine stabilizes the agonist-induced desensitized state(s) of the AChR. This was observed by the decrease of the cluster frequency in both cell-attached and outside-out patches at high ACh concentrations.

A similar effect as the one described for adiphenine at the macroscopic level has been observed for fipronil on GABA$_A$ receptors (Li and Akk, 2008). The most probable mechanism suggested by the authors is a long-lived blockade of the open state. The relative slow desensitization of this receptor allows studies of inhibition and recovery during the decay of the current, which is not easy in our experiments due to the faster desensitization rate (0.17 vs. 50 $s^{-1}$ for GABA$_A$ receptor and AChR respectively). However at the single-channel level fipronil does not decrease the mean open time, as observed for adiphenine.

### Binding site for proadifen and adiphenine

Meproadifen has been shown to label $\alpha E262$ in *T. californica* AChR (Pedersen *et al.*, 1992). We found that the mutation $\alpha E262K$ did not affect the action of proadifen on adult mouse muscle AChR but inhibition by adiphenine was significantly decreased. This result agrees with our competition experiments, which showed that proadifen does not affect the inhibition by adiphenine. Therefore, the binding site for the two drugs may be different in the adult mouse muscle AChR, accounting for the differences observed in the mechanisms of action. It has been recently shown that a photoactivatable analogue of octanol, 3-azioctanol, causes irreversible loss of function due to the stabilization of a desensitized state by binding to $\alpha E262$ in foetal mouse AChR (Forman *et al.*, 2007). Therefore, this residue may be a common target for NCIs that act by enhancing desensitization from the open state.

Although local anaesthetics have commonly been accepted to inhibit AChR activity by acting as fast open-channel blockers (Gentry and Lukas, 2001; Arias and Blanton, 2002), our results show that it is not the only way by which they act, and reveal that when analysed in detail channel inhibition is highly complex. The IC$_{50}$ values determined here for proadifen and adiphenine are in the order of the therapeutic

concentrations of clinically used local anaesthetics attainable in blood (Clarke, 1986). Therefore, it is possible that these drugs also alter the function of AChRs.

## Acknowledgements

## Conflict of interest

None.

## References

Alexander SPH, Mathie A, Peters JA (2008). Guide to Receptors and Channels (GRAC), 3rd edn (2008 revision). *Br J Pharmacol* **153** (Suppl. 2): S1–S209.

Aracava Y, Albuquerque EX (1984). Meproadifen enhances activation and desensitization of the acetylcholine receptor-ionic channel complex (AChR): single channel studies. *FEBS Lett* **174**: 267–274.

Arias HR, Blanton MP (2002). Molecular and physicochemical aspects of local anaesthetics acting on nicotinic acetylcholine receptor-containing membranes. *Mini Rev Med Chem* **2**: 385–410.

Arias HR, Bhumireddy P, Bouzat C (2006). Molecular mechanisms and binding site locations for noncompetitive antagonists of nicotinic acetylcholine receptors. *Int J Biochem Cell Biol* **38**: 1254–1276.

Auerbach A, Akk G (1998). Desensitization of mouse nicotinic acetylcholine receptor channels. A two-gate mechanism. *J Gen Physiol* **112**: 181–197.

Bouzat C, Bren N, Sine SM (1994). Structural basis of the different gating kinetics of fetal and adult acetylcholine receptors. *Neuron* **13**: 1395–1402.

Bouzat C, Roccamo AM, Garbus I, Barrantes FJ (1998). Mutations at lipid-exposed residues of the acetylcholine receptor affect its gating kinetics. *Mol Pharmacol* **54**: 146–153.

Bouzat C, Barrantes FJ, Sine SM (2000). Nicotinic receptor fourth transmembrane domain: hydrogen bonding by conserved threonine contributes to channel gating kinetics. *J Gen Physiol* **115**: 663–672.

Bouzat C, Gumilar F, Esandi MC, Sine SM (2002). Subunit-selective contribution to channel gating of the M4 domain of the nicotinic receptor. *Biophys J* **82**: 1920–1929.

Boyd ND, Cohen JB (1984). Desensitization of membrane-bound *Torpedo* acetylcholine receptor by amine noncompetitive antagonists and aliphatic alcohols: studies of [3H]acetylcholine binding and 22Na+ ion fluxes. *Biochemistry* **23**: 4023–4033.

Catterall WA, Mackie K (2001). Local anaesthetics. In: Hardman JG, Limbird LE, Gilman AG (eds). *Goodman & Gilman's the Pharmacological Basis of Therapeutics*. McGraw-Hill Profesional: New York, pp. 367–384.

Changeux JP, Taly A (2008). Nicotinic receptors, allosteric proteins and medicine. *Trends Mol Med* **14**: 93–102.

Clarke EGC (1986). Analytical and toxicological data: monographs. In: Moffat AC, Jackson JV, Moss MS, Widdop B (eds). *Clarke's Isolation and Identification of Drugs in Pharmaceuticals, Body Fluids and Post-Mortem Material*. The Pharmaceutical Press: London, pp. 307–1069.

Corradi J, Spitzmaul G, De Rosa MJ, Costabel M, Bouzat C (2007). Role of pairwise interactions between M1 and M2 domains of the nicotinic receptor in channel gating. *Biophys J* **92**: 76–86.

Demazumder D, Dilger JP (2001). The kinetics of competitive antagonism by cisatracurium of embryonic and adult nicotinic acetylcholine receptors. *Mol Pharmacol* **60**: 797–807.

Dilger JP, Brett RS (1990). Direct measurement of the concentration- and time-dependent open probability of the nicotinic acetylcholine receptor channel. *Biophys J* **57**: 7223–7731.

Dilger JP, Liu Y (1992). Desensitization of acetylcholine receptors in BC3H-1 cells. *Pflugers Arch* **420**: 479–485.

Elenes S, Auerbach A (2002). Desensitization of diliganded mouse nicotinic acetylcholine receptor channels. *J Physiol* **541**: 367–383.

Forman SA (1999). A hydrophobic photolabel inhibits nicotinic acetylcholine receptors via open-channel block following a slow step. *Biochemistry* **38**: 14559–14564.

Forman SA, Zhou QL, Stewart DS (2007). Photoactivated 3-azioctanol irreversibly desensitizes muscle nicotinic ACh receptors via interactions at alphaE262. *Biochemistry* **42**: 11911–11918.

Gentry CL, Lukas R (2001). Local anaesthetics noncompetitively inhibit function of four distinct nicotinic acetylcholine receptor subtypes. *J Pharmacol Exp Ther* **299**: 1038–1048.

Gumilar F, Arias HR, Spitzmaul G, Bouzat C (2003). Molecular mechanisms of inhibition of nicotinic acetylcholine receptors by tricyclic antidepressants. *Neuropharmacol* **45**: 964–976.

Hamill OP, Marty A, Neher E, Sakmann B, Sigworth FJ (1981). Improved patch-clamp techniques for high-resolution current recording from cells and cell-free membrane patches. *Pflugers Arch* **391**: 85–100.

Heidmann T, Oswald RE, Changeux JP (1983). Multiple sites of action for noncompetitive blockers on acetylcholine receptor rich membrane fragments from *Torpedo* marmorata. *Biochemistry* **22**: 3112–3127.

Imoto K, Busch C, Sakmann B, Mishina M, Konno T, Nakai J *et al.* (1988). Rings of negatively charged amino acids determine the acetylcholine receptor channel conductance. *Nature* **335**: 645–648.

Li P, Akk G (2008). The insecticide fipronil and its metabolite fipronil sulphone inhibit the rat α1β2γ2δL GABA$_A$ receptor. *Br J Pharmacol* **155**: 783–794.

Liu Y, Dilger JP (1991). Opening rate of acetylcholine receptor channels. *Biophys J* **60**: 424–432.

Lurtz MM, Pedersen SE (1999). Aminotriarylmethane dyes are high-affinity noncompetitive antagonists of the nicotinic acetylcholine receptor. *Mol Pharmacol* **55**: 159–167.

Maleque MA, Souccar C, Cohen JB, Albuquerque EX (1982). Meproadifen reaction with the ionic channel of the acetylcholine receptor: potentiation of agonist-induced desensitization at the frog neuromuscular junction. *Mol Pharmacol* **22**: 636–647.

Miyazawa A, Fujiyoshi Y, Unwin N (2003). Structure and gating mechanism of the acetylcholine receptor pore. *Nature* **423**: 949–955.

Papke RL, Oswald RE (1989). Mechanisms of noncompetitive inhibition of acetylcholine-induced single-channel currents. *J Gen Physiol* **93**: 785–811.

Pedersen SE, Sharp SD, Liu WS, Cohen JB (1992). Structure of the noncompetitive antagonist-binding site of the *Torpedo* nicotinic acetylcholine receptor. [3H]meproadifen mustard reacts selectively with alpha-subunit Glu-262. *J Biol Chem* **267**: 10489–10499.

Prince RJ, Sine SM (1999). Acetylcholine and epibatidine binding to muscle acetylcholine receptors distinguish between concerted and uncoupled models. *J Biol Chem* **274**: 19623–19629.

Ryan SE, Blanton MO, Baenziger JE (2001). A conformational intermediate between the resting and desensitized states of the nicotinic acetylcholine receptor. *J Biol Chem* **276**: 4796–4803.

Sakmann B, Patlak J, Neher E (1980). Single acetylcholine-activated

channels show burst-kinetics in presence of desensitizing concentrations of agonist. *Nature* **286**: 71–73.

Salamone FN, Zhou M, Auerbach A (1999). A re-examination of adult mouse nicotinic acetylcholine receptor channel activation kinetics. *J Physiol* **516**: 315–330.

Sine SM, Engel AG (2006). Recent advances in Cys-loop receptor structure and function. *Nature* **440**: 448–455.

Spitzmaul G, Dilger JP, Bouzat C (2001). The noncompetitive inhibitor quinacrine modifies the desensitization kinetics of muscle acetylcholine receptors. *Mol Pharmacol* **60**: 235–243.

Wenningmann I, Dilger JP (2001). The kinetics of inhibition of nicotinic acetylcholine receptors by (+)-tubocurarine and pancuronium. *Mol Pharmacol* **60**: 790–796.